ANALYSIS OF MULTIGRID EXTRACTION PLASMA MENISCUS FORMATION

M. Cavenago*, INFN-LNL, V. Antoni, F. Sattin, CNR/RFX, Padova, A. Tanga , MPI/IPP, Garching

Abstract

Negative ion source for spallation sources or neutral beam injectors (NBI) for tokamaks requires carefully matched electric and magnetic fields in the beam formation area due to the presence of three species of particles: the collisional and fully magnetized electrons; the slightly magnetized positive ions; the negative ions, formed within few cm from plasma-beam interface (meniscus). As a step towards a collisional and magnetized theory for a charged fluid in a realistic 2D or 3D geometry, a 1D model based on a Vlasov equation with a collision operator is written and discussed in detail. A closed equation is obtained for the forward directed current; its solution in modes and formulas for density n are given.

INTRODUCTION

Negative hydrogen ion sources are typically envisioned for high intensity application: single aperture 35 mA beam for synchrotron multiturn injection (H^- can be injected with a stripping foil) and multiaperture source, for producing 1 MeV 40 A beams required for tokamak heating and current driving[1, 2]. Development of simulation codes for single aperture sources is well debated in the literature and based on one dimensional modelling of presheath and microscopic sheath formation [2, 3, 4]. Even if beam formation is similar in multiaperture sources, design is also constrained by the limited space available for the magnetic filter system (Fig. 1). It is also interesting to study 2D effects of plasma-beam interface (meniscus) with charged fluid models (that is $\triangle\phi = F[\phi]$ where F is a functional, reasonably simple, of the electrostatic potential ϕ) because: 1) at least three different charged fluid can be recognised: the H-, produced within few cm from meniscus, the electrons and the positive ions; 2) different magnetic filters need to be compared; 3) optimization of electron dump and outlet electrodes strongly depends on plasma preasheath properties and on meniscus. Improvement of beam simulation tools and of understanding of underlying plasma physics is likely to be in increasing demand, in view of its potential help to improve source performance and impact on related engineering issues; for example, electron beam loss on multigrid system determines cooling requirements. In this paper, we study the effect on the charge distribution of ions and electrons of plasma conditions where both collision and applied magnetic and electric field are important.

A typical multigrid [5] geometry is shown in Fig. 1. Negative H^- are formed: 1) in the plasma volume near the source extraction holes (typical path length for H^- neutralization λ_n is few cm), provided electron temperature T_e (in energy unit) is sufficiently low ($T_e \cong 1$ eV) and an abundant supply of H_2 molecules with vibration levels excited is coming from inner plasma regions [1]; 2) on Cesium covered walls near the extraction. Even if the mechanism 2 is more efficient, preliminary tracking simulation shows that a fine tuning of the electrostatic potential ϕ and magnetic field $\mathbf{B}$ is needed for extraction [6].

Let z be the beam axis direction, with $z = 0$ the plasma grid (in following 1D model, $z = 0$ will be the plasma boundary and $z < 0$ the plasma region). For numerical examples, we assume a total positive ion density $n_+ \cong 10^{17}$ m^{-3}, while the total H_2 density is about 10^{20} m^{-3} (0.41 Pa at room temperature).

We find two permanent magnet systems, the extraction filter (bar longer axis y) and the inner filter (usually crossed, with axis x). The former filter with middle plane $z = z_e \cong 10$ mm and periodicity $d \cong 25$ mm generates a vector potential component $A_y(x, z)$, with a peak $A_y \cong 500$ G cm at z_e. Typically $B_x \cong 30$ to 100 G at $z = 0$ and $|B_x|$ peaks in the extraction gap; this filter has the main purpose of steering the residual electron current (with density j_e) away from the axis and against the extraction grid, leaving the ions (of current density j_{H^-}) with a direction substantially unaffected ($\int B_x \mathrm{d}z = 0$). The inner filter with midplane z_f (typically $z_f \cong -50$ mm) and a $B_f = 50$ G peak has the purpose of weakening the flow of warm electrons with $T_e \cong 3$ eV [1] from the inner plasma to the H^- production region, since they effectively dissociate H^-. Requesting that the collision frequency of electrons $\nu_{ei} = k_e n_e / T_e^{3/2}$ with $k_e = 6.3 \times 10^{-11}$ m^3 eV$^{3/2}$/s be greater than the cyclotron frequency gives a condition

$$E_e = \frac{3}{2} T_e \leq \frac{3}{2} \left(\frac{k_e n_e m}{e B_f} \right)^{2/3} \cong 0.1\mathrm{eV} \qquad (1)$$

for the efficient transmission of electrons to the H^- production area. Then, even considering filter imperfection and heating by ion collisions and by potentials, $T_e \cong 1$ eV is easily attained in H^- production region.

Let $\phi = 0$ on the plasma grid; ϕ is determined by

$$\triangle\phi = -(e/\varepsilon_0)(n_{H+} - n_e - n_{H-})[\phi] \qquad (2)$$

(where the functional dependence of n from ϕ is put in evidence) and by the selfconsistently determined plasma potential ϕ_p [6] and by the extraction grid positive potential V_{ext}, which also controls the plasma-beam interface position. In the H^- sources, we expected a comparatively deep penetration of the positive potential since electrons are rapidly accelerated to form a beam and the magnetic field $\mathbf{B}$ is weak at $z = 0$. Anyway a detailed balance of

* cavenago@lnl.infn.it, INFN-LNL, Legnaro (PD) Italy

effects of $\mathbf{B}$, of collision and of ϕ is necessary for quantitative analysis and is outlined later. It should be noted some degree of $V_{\rm ext}$ shielding is provided by electrode geometry (non-Pierce plasma electrode angles [4], hole depth).

In positive ion source or in collisionless and $B = 0$ plasma models, n_{H+} reduces to well-known expressions of ϕ and of v_{zi}, the assumed ion initial velocity at $z = z_i$: $n(z) = \frac{1}{2} n(z_i) v_{zi} / \sqrt{v_{zi}^2 + (2e/m)[\phi(z_i) - \phi(z)]}$ and similarly for the electrons in the beam. Plasma electrons are instead considered completely thermalized (see Ref. [7] for some discussion of this), so that $n_e(z) = n_0 \exp(e\phi(z)/T_e)$. Both n dependencies are local, so that eq. 2 can be still solved as a standard (even if nonlinear) partial differential equation. On the contrary, considering collision and magnetic field we generally find n to depend globally on ϕ; integro-differential equations for n and j will be approximately solved by eq. 18, introducing a mode decomposition and giving a relation $n[\phi]$ similar to local ones.

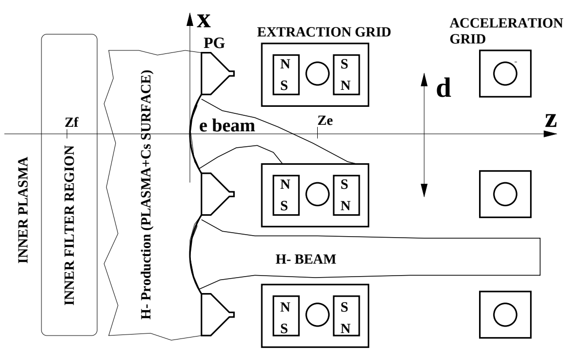

Figure 1: Typical extraction geometry (not to scale): PG = plasma grid; circles are cooling water channels

KINETIC EQUATIONS

For fig. 1 geometry a 2D model, where y coordinate is ignorable, is well appropriate. Moreover for the central part of each hole, where penetration of $V_{\rm ext}$ is deeper, $B_z = \partial_x A_y \cong 0$ and $E_x \cong 0$ so that no x variation of A_y and ϕ need to be considered in first approximation, obtaining a 1D model. Similarly we assume $A_x = 0$ (thus the inner filter region is ignored, or inner filter is considered aligned with extraction filter). The phase space distribution f is integrated on x, P_x, so that it depends only on z and momenta $\tilde{P}_y$ (canonical and invariant of the motion) and $\tilde{p}_z$; we assume a common background temperature T (for example 1 eV) for the three species. The normalized hamiltonian $h = H/T$ is

$$h(z, p_z; P_y) = \tfrac{1}{2} p_z^2 + \tfrac{1}{2}(P_y - a(z))^2 + v(z) \qquad (3)$$

with the normalized momenta $P_y = \tilde{P}_y/\sqrt{mT}$ and $p_z = \tilde{p}_z/\sqrt{mT}$ and fields $v = e\phi/T$ and $a = eA_y/\sqrt{mT}$ for protons (for H$^-$ or electron change sign and/or mass). For example if $A_y = -10^{-4}$ T m and $\phi = -1$ V, we get $a \cong v \cong -1$ for protons (respectively 1 for H$^-$ and $a \cong 40$, $v \cong 1$ for electrons). The collisional Vlasov equation for $f(z, p_z; P_y)$ is

$$p_z \frac{\partial f}{\partial z} - \frac{\partial h}{\partial z}\frac{\partial f}{\partial p_z} = \frac{1}{\sqrt{T/m}} \mathrm{d}_t f|_c \qquad (4)$$

In order to decouple the three species and for the sake of simplicity, a collisional operator $\mathrm{d}_t f|_c$ for fixed scatterers is assumed, so that: 1) mean free path length along z is a constant λ_i; 2) scattered distribution is isotropic [8] and maxwellian with temperature T; in other words for electron we neglect that energy relaxation time is much greater than momentum relaxation time according to classical theory; this incorporates any anomalous electron energy relaxation [7, 9]. We have

$$\frac{1}{\sqrt{T/m}} \mathrm{d}_t f|_c = \frac{|p_z|}{\lambda_i} \left\{ -f + \frac{g(p_z)}{c_1} g(P_y - a) \int' |p_z| f \right\} \qquad (5)$$

where $\int' = \int \mathrm{d}p_z \mathrm{d}P_y$ and $g(x) = \exp(-x^2/2)/\sqrt{2\pi}$ and $c_1 = \int \mathrm{d}x\, |x| g(x) = \sqrt{2/\pi}$.

Let us separate the current in forward z-direction j^+ as

$$j^+ = \int^+ p_z f \quad , \quad j^- = -\int \mathrm{d}P_y \int_{-\infty}^0 \mathrm{d}p_z p_z f \qquad (6)$$

with $\int^+ = \int \mathrm{d}P_y \int_0^\infty \mathrm{d}p_z$. Note that $j \equiv j^+ - j^-$ satisfies $\partial j/\partial z = 0$; and that $j_\Sigma \equiv j^+ + j^- = 2j^+ - j$. Applying $\int^+$ to equation 4 we get:

$$\frac{\partial j^+}{\partial z} = -\frac{j}{2\lambda_i} - \int \mathrm{d}P_y \frac{\partial h}{\partial z} f(z, 0; P_y) \qquad (7)$$

where the first term is the net balance of collisions and the second the change of j^+ due particle turning point $p_z = 0$.

For $p_z > 0$, using the orbit integration and recognizing that $\int' |p_z| f = j_\Sigma$ in the collisional operator and using the shorthand $\eta_y = P_y - a(z')$, we get

$$f = \int_\alpha^z \mathrm{d}z' \mathrm{e}^{\frac{-|z'-z|}{\lambda_i}} \frac{j_\Sigma}{2c_1\lambda_i} \int_0^\infty \mathrm{d}p_z' |p_z'| \delta(h' - h) g(\eta_y) g(p_z') \qquad (8)$$

where α is the lower plasma boundary and the prime indicates quantities at a point on the orbit with the final point z, not a derivative. The Dirac's delta makes sure that p_z' is consistent with the final p_z; in detail, the condition $h' - h = 0$ is

$$\eta_z^2 + 2\bar{a}\eta_y + 2b - p_z^2 = 0 \qquad (9)$$

with $\eta_z = p_z'$ and $\bar{a} = a(z) - a(z')$ and $b = -\frac{1}{2}(\bar{a})^2 - \bar{v}$ and $\bar{v} = v(z) - v(z')$. For $p_z < 0$, eq. 8 is similar, with the integration range $[\beta, z]$ and β the upper plasma boundary. Double turning point orbits are suppressed by collisions.

Observing that $\partial_z \Theta(h' - h) = -\partial h/\partial z\, \delta(h' - h)$ and defining

$$M^1(\bar{a}, \bar{v}) = \frac{2}{c_1} \int^+ \eta_z \Theta(\eta_z^2 + 2\bar{a}\eta_y + 2b) g(\eta_z) g(\eta_y) \qquad (10)$$

0-7803-8859-3/05/$20.00 ©2005 IEEE

with b as in eq. 9, Θ the Heaviside function and now $\int^+ = \int d\eta_y \int_0^\infty d\eta_z$, eq. 7 becomes

$$\frac{\partial j^+}{\partial z} + \frac{j}{2\lambda_i} = \int_\alpha^\beta dz' e^{\frac{-|z'-z|}{\lambda_i}} \frac{j_\Sigma}{2\lambda_i} \frac{\partial M^1}{\partial z} \quad (11)$$

which is a closed equation for j^+. After its solution for j^+ is found as modes $j^+ = j_q \exp(qz/\lambda_i)$, n may be easily computed integrating eq. 8. Indeed, defining

$$N(\bar{a}, \bar{v}) = \int_0^\infty dp_z\, \partial M^1(\bar{a}, \bar{v} + \tfrac{1}{2}p_z^2)/\partial p_z^2 \quad (12)$$

(the p_z^2 derivative matches the Dirac's delta in eqs. 8) and

$$Z^p(k_u) = \int_0^\infty du\, e^{k_u u/\lambda_i} N(a(z) - a(z'), \bar{v}) \quad (13)$$

with $p = \pm 1$, where $z' = z - pu$ is also inside v, we have

$$n = -j\frac{Z^{-1}(-1) + Z^1(-1)}{2\lambda_i} + j_q e^{\frac{qz}{\lambda_i}} \frac{Z_\Sigma}{\lambda_i} \quad (14)$$

with $Z_\Sigma = Z^{-1}(-1+q) + Z^1(-1-q)$.

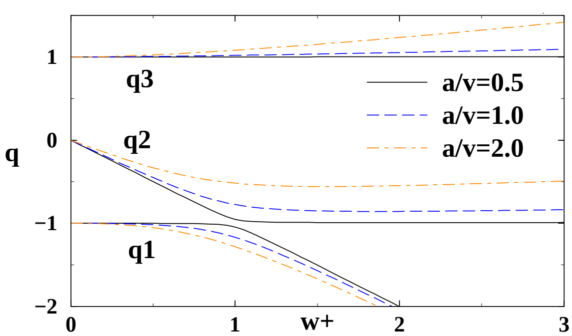

Figure 2: Solution for mode equation

Modes

Expanding $\bar{v} = v_1(z - z') + O(z - z')^2$ where $v_1 = -eE_z/T$ and similarly $\bar{a} \cong a_1(z - z')$, we express both as function of $s \equiv v_1(z - z')$; in detail $\bar{a} = 2^{-1/2}c_1 s$ where $c_1 = 2^{1/2}a_1/v_1$. The M^1 exact expression

$$M^1 = \tfrac{1}{2}\mathrm{erfc}\frac{\bar{a}^2 + \bar{v}}{|\bar{a}|\sqrt{8}} + \tfrac{1}{2}e^{-\bar{v}}\mathrm{erfc}\frac{\bar{a}^2 - \bar{v}}{|\bar{a}|\sqrt{8}} \quad (15)$$

with $\mathrm{erfc}(x) = 1 - \Phi(x)$ and Φ the error function, is then easily plotted as a function of s for several c_1 and is apparently well approximated by $\exp(m_- s)$ for $s < 0$ and by $\exp(-m_+ s)$ for $s > 0$ with coefficient $m_\pm = (c_c \pm 1)/2$ and

$$c_c(c_1) = c_1\pi^{-1/2}e^{-1/c_1^2} + \Phi(1/c_1) \quad (16)$$

We discuss the case $v_1 > 0$ (retarding field for proton) only, for simplicity. Substituting in the eq. 11 the trial solution $j^+ = j_0 + j_q \exp(qz/\lambda_i)$, we extend the plasma range $[\alpha, \beta]$ to $-\infty, +\infty$ to simplify results of $\exp(-m_+ s)$ integration in eq. 11. We find $j_0 = j(1+L_0)/(2L_0)$ where $L_0 = \int dz e^{\frac{-|s|}{v_1\lambda_i}} \partial_z M^1 = (w^- - w^+)/(1+w^-)(1+w^+)$ with

$$w^+ = v_1\lambda_i(c_c + 1)/2 \quad , \quad w^- = v_1\lambda_i(c_c - 1)/2 \quad (17)$$

and the growth rate q satisfies the third degree equation:

$$q = -\frac{w^+}{1 + w^+ + q} + \frac{w^-}{1 + w^- - q} \equiv G(q) \quad (18)$$

A simple graphical study of $G(q) - q$ shows that all roots q_i are real and bounded, namely

$$-1-w^+ < q_1 \le -1 \le q_2 < 0, \quad 1 \le q_3 < 1+w^- \quad (19)$$

When $w^- \to 0$, $q_3 \to 1$ and the other two solutions are $-1, -w^+$; in general q_i are near to this values (see fig. 2 plot). The solution near to $-w^+$, named q_m, is particularly interesting, since it is similar to a Maxwellian factor; note indeed that

$$\log(j - j_0)_{,z} = \frac{q_m}{\lambda_i} \cong -\frac{e\phi_{,z}(1 + c_c)}{2T} \equiv -\frac{eW,z}{T} \quad (20)$$

where $_{,z}$ is z-derivative and W an effective potential; we get $W = \frac{1}{2}\int dz[\phi, z + (\phi_{,z}^2 + 2B_x^2 T/(\pi m)]$ approximating c_c for $c_1 \ge 1$. Moreover, a simple estimate gives

$$N = \sqrt{\pi/2}\, e^{-\bar{v}}\mathrm{erfc}\Big(\Re\Big[\sqrt{\tfrac{1}{2}(\bar{a})^2 - \bar{v}}\Big]\Big) + O(\bar{a}^2) \quad (21)$$

where $\Re$ is the real part, but it loses accuracy for large a_1. Using it in eq. 13, for $p = 1$ we find $\bar{v} \cong v_1 u$ and thus $Z^+ = c_8/(v_1 - k_u)$ with $c_8 = (\pi/8)^{1/2}$; expression for Z^{-1} is slightly complicate. From eq. 14, we get

$$n_{H+} = -\frac{jc_8}{2}\left(\frac{1}{1+\sqrt{w_0}} + \frac{1}{1+w_0}\right) +$$

$$\frac{j_q c_8}{e^{zw^+/\lambda_i}}\left(\frac{1}{1 + w^+ + \sqrt{(1+w^+)w_0}} + \frac{1}{1+w^-}\right) \quad (22)$$

with $w_0 = v_1\lambda_i$, showing attenuation of the density (up to a possible breaking point $n = 0$). Similar expression can be derived for the other modes, so that the expectation of decreasing proton density is confirmed. More work is needed to include finite boundaries in eq. 11 and, more important, to investigate the effects of eq. 22 and similar n in eq. 2.

REFERENCES

[1] R. Zorat, D. Vender, J. Phys. D, 33 (2000) 1728
[2] R. F. Welton et al., Rev. Sci. Instrum. 73 (2002), 1013
[3] M. Bacal et al., Rev. Sci. Instrum. 71 (2000) 1082
[4] R. Becker, Rev. Sci. Instrum. 75 (2004), 1687
[5] W. Kraus et al., Rev. Sci. Instrum. 75 (2004), 1832
[6] F. Sattin et al., to be submitted to Nuclear Fusion
[7] H. Schmitz et al. , Phys. Plasmas, 3 (1996), 2486
[8] P. M. Morse, H. Feshbach, Methods of Theoretical Physics, McGraw-Hill, New York, 1953
[9] A. T. Forrester, Large Ion Beams, John Wiley, NY, 1996